21st Australasian Fluid Mechanics Conference
Adelaide, Australia
10-13 December 2018

Effect of Particle Loading on Interference in Planar Laser Induced Fluorescence Thermometry

E. W. Lewis[1,3], T. C. W. Lau[1,3], Z. W. Sun[1,3], G. J. Nathan[1,3] and Z. T. Alwahabi[2,3]

[1]School of Mechanical Engineering
The University of Adelaide, South Australia 5005, Australia

[2]School of Chemical Engineering
The University of Adelaide, Adelaide, South Australia 5005, Australia

[3]Centre for Energy Technology
The University of Adelaide, Adelaide, South Australia 5005, Australia

Abstract

Planar laser-induced fluorescence (PLIF) of toluene has been applied to measure the gas-phase temperature in a particle-laden jet heated to controlled gas temperatures between 20°C $\leq T \leq$ 120°C. This method utilises the dependence on temperature of the spectral emission of toluene vapour when excited at a wavelength of 266 nm. Single-shot, planar imaging of temperature was achieved with a high signal-to-noise ratio from the ratio of the fluorescent emissions at two wavelength bands that are recorded simultaneously with two intensified CCD cameras, after first correcting for spatial variations in camera efficiency. The effects of interference from particles and laser sheet attenuation on the accuracy of the PLIF thermometry method was investigated for 40 μm PMMA particles, with the volume loading varied in the two-way coupling regime. Reliable measurements were achieved into the two-way coupling regime.

Introduction

Heat transfer within particle-laden flows is relevant to a wide range of industrial processes, including in pulverized fuel burners, for mineral processing plants in which the feedstock is processed as a powder [15], and in concentrated solar thermal particle receivers (or reactors), in which the particles act as the absorbing medium for incident radiation [4]. In these systems, there are strong temperature gradients between the particles and surrounding gas flows, either due to chemical reactions or the absorption of high flux concentrated radiation. Particle volume loading, defined as: $\phi_v = \dot{V}_p/\dot{V}_f$, where $\dot{V}_p$ is the volume flow rate of particles and $\dot{V}_f$ the volume flow rate of the fluid, is a common parameter used to characterise particle-laden systems [2]. Of interest due to its applicability in industrial flows is the two-way coupling regime, which includes flows with volume loadings between 10^{-6} and 10^{-3}. In these systems, particle-fluid dynamics affect heat transfer, with the local particle and gas properties including temperature, velocity and concentration significant [12]. To optimize particle-laden flow processes, there is a need to understand particle-fluid heat transfer. This, in turn, requires knowledge of the temperature of both phases.

Heat transfer in particle-laden flows depends on the gradients in temperature, including that between phases, together with those in velocity and concentration, all of which vary in time and space in a turbulent flow [10]. Various methods to measure the temperature of the gas phase have been developed, including the single point methods of cold-wire anemometry [1] and thermocouples together with laser based methods such as Rayleigh scattering [8], coherent anti-Stokes Raman scattering (CARS) [13] and planar laser-induced fluorescence (PLIF) [14]. However, these methods are typically poorly suited to application in the presence of particles, which either lead to blockage of probes or optical interference due to their strong scattering interference. Of the available methods for measurement of the gas-phase temperature in particle-laden flows, PLIF can be deduced to offer good potential, as it is a spatially resolved method in which the temperature signal can be separated from the scattering of particles with optical filtering [14]. However, to date, no previous investigation has been performed on the influence of volumetric loading of particles on the level of interference, and hence on accuracy of the gas phase temperature measurement. For this reason, the aim of the present investigation is to meet this need.

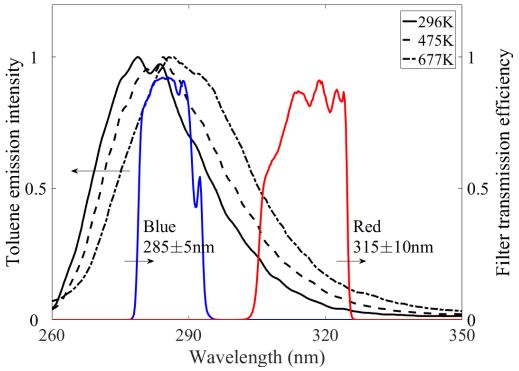

Figure 1: Normalised toluene fluorescent emission spectrum at different temperatures (adapted from [3]) and optical filter transmission efficiencies of the fluorescence cameras

The PLIF method measures the fluorescence signal from a tracer in the gas flow. The signal is measured with a camera, which captures the intensity of fluorescent emissions of the tracer after excitation by a laser formed into a thin sheet to allow for spatially resolved measurements. The intensity of fluorescent emissions from a tracer excited by a laser is dependent on the intensity of the laser (I_{laser}), the tracer number density (n), the absorption cross section of the tracer (σ), the fluorescence quantum yield of the tracer (ψ), the collection solid angle (Ω) and quantum efficiency of detection (η), which vary with spatial location (x, r), local temperature (T), excitation wavelength (λ), pressure (p) and system optics [3]. The fluorescing intensity is given by:

$$I_{LIF} = I_{laser}\Omega\eta n(x,r)\sigma(\lambda, T(x,r))\psi(\lambda, T(x,r), p) \qquad (1)$$

In the event that laser fluence and number density of the tracer are kept constant in the measurement region, it can be shown that the fluorescent intensity at any location in the flow will be dependent on temperature only [11]. However, a flow with constant number density can only be achieved when mixing is absent or controlled, which is not the case in turbulent,

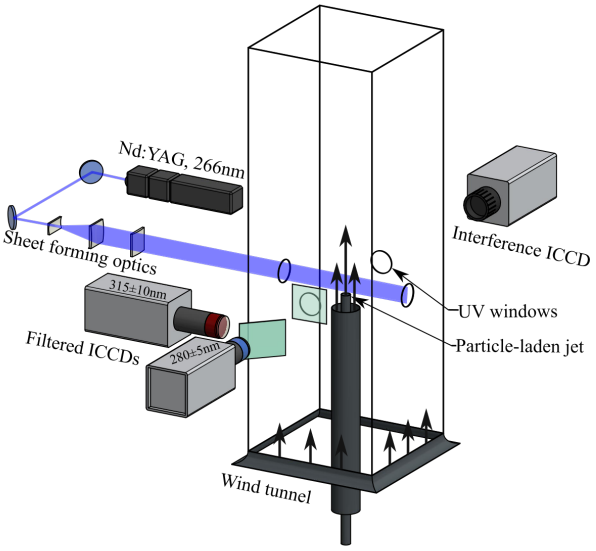

Figure 2: Experimental setup for two-colour LIF thermometry of particle-laden jets

particle-laden flows. Two-colour LIF thermometry is an alternate method in which fluorescent emissions are imaged in two wavelength bands. The ratio of the signal in these bands is a function of temperature only, as all spatial location and pressure effects cancel out, and wavelength dependent parameters are constant [11]. The wavelength bands collected are termed the red and blue channels, where the red channel images the fluorescence emissions at longer wavelengths than the blue. The temperature can be represented by the equation: $T(x,r) = f(I_{red}/I_{blue})$, where I_{red} and I_{blue} are the intensity signals collected in the two spectral regions. The function f can be determined by calibration under experimental conditions.

Methodology

Toluene was chosen as the fluorescent tracer, because its emission has a high sensitivity to temperature and a high signal strength in the target range of 280-700 K. Toluene can be excited by a single UV laser, commonly at the wavelengths of 248 nm or 266 nm. The red shift of the emission spectrum of toluene with increasing temperature is shown in Figure 1 [3]. The measurements were taken in nitrogen because the emission intensity of toluene is much greater in nitrogen than air, due to quenching by oxygen [7].

Jet Flow Setup

The PLIF method was tested in a pipe jet with internal diameter (D) of 6.23 mm and a 69 mm coaxial annular flow, both run with nitrogen, as shown in figure 2. The jet pipe was centrally located in a 300 mm square wind tunnel, with the tunnel co-flow conditioned by a honeycomb section and screens to provide a uniform co-flow. The jet pipe was sufficiently long ($L/D = 176$) for the particle-laden flow to approach the fully developed condition [9], and was heated with an electrical heated tape to temperatures of 20°C or 120°C, although temperatures of up to 220°C can be achieved. The flow rate through the jet was controlled by a mass flow meter to be fully turbulent with a Reynolds number of 5000. Here, the Reynolds number is defined by: $Re = \rho VD/\mu$, where ρ is the flow density, V is the bulk mean velocity of the jet, D is the pipe diameter and μ is the dynamic viscosity of the flow. The particles used were PMMA

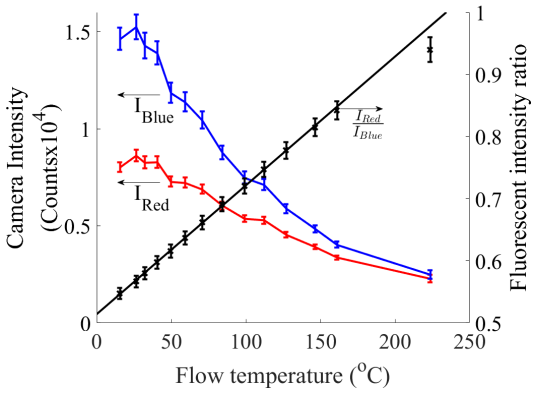

Figure 3: Calibration data for intensity ratio of a toluene seeded heated jet. The solid line shows a curve fitted to the data. Also shown is the average camera counts for the red and blue channels. Error bars are one standard deviation either side of the mean.

(Microbead spheromers) with a mean diameter of 40 μm, and standard deviation under 5%. The particles were introduced into the flow by a screw feeder rotating at a constant speed located in an airtight enclosure. The screw feeder provides an average ϕ_v of 4×10^{-4}, leading to a flow in the two-way coupling region. Toluene was seeded in the flow by bubbling nitrogen through a toluene reservoir. The concentration of toluene in the flow was approximately 2.75% by volume, corresponding to saturation at room temperature.

Laser and Imaging System

A Quantel Q-smart Nd:YAG laser at the fourth harmonic (266 nm) was used to excite toluene in the particle-laden flow. The laser beam was formed into a thin sheet using three cylindrical lenses. The sheet was 40 mm high and approximately 0.5 mm thick through measurement region. The fluorescence signals were collected using two Princeton instruments PI-Max4 ICCD cameras, with the image focused by a single spherical lens (f =100 mm). The camera gate opened 20 ns before the laser pulse and remained open for 220 ns to collect the strongest fluorescent emission while minimizing the effect of interference. The emissions were initially filtered by two 275 nm long-pass filters (Asahi Spectra ZUL0275) to remove scattered light. The fluorescent emission was then split with a dichroic beam-splitter (Semrock FF310-Di01) into blue and red channels, as shown in figure 2. The transmission efficiencies of the blue and red channel are shown in Figure 1, where the blue channel images in the region of 285±5 nm, and the red channel images in the region of 315±10 nm. The blue channel was collected through a 272 nm long-pass filter (Semrock FF01-272/LP) and a 280 nm bandpass filter (Semrock FF01-280/20), and the red channel was collected through a 300 nm long-pass (Semrock FF01-300/LP) and 330 nm short-pass filter (Semrock FF01-330/SP). The filters were chosen to measure spectral regions with a good sensitivity to changes in temperature and to suppress scattered laser light.

The interference from particles was imaged with a HSFC pro ICCD camera through a Nikon lens (f =50 mm, F/1.4). The particle volume loading was inferred from the intensity of the interference signal, which was possible because the particles are monodisperse, and the laser power was known. The scattered signal also provides a measure of the interference, since this is proportional to laser power, particle number density and the particle diameter squared. Since the shot-by-shot laser power

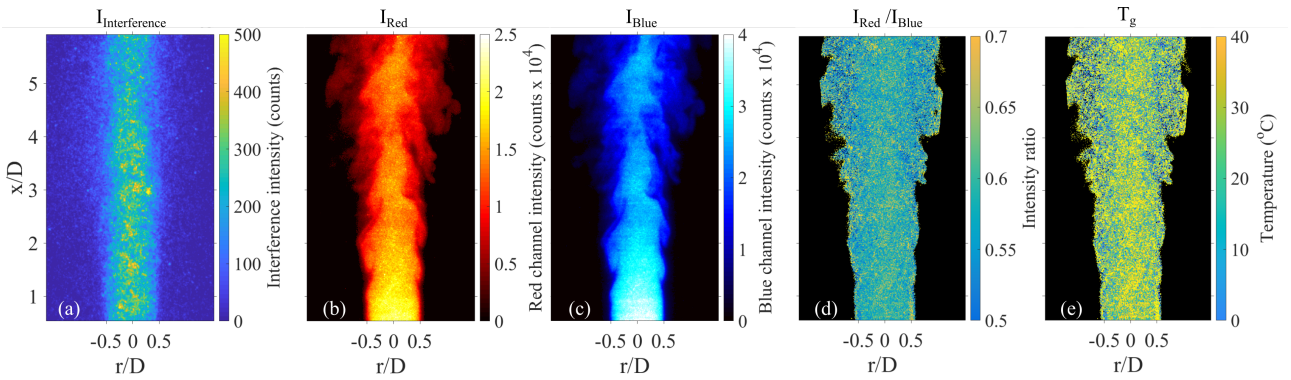

Figure 4: Images used in processing - (a) is a single-shot particle interference image, (b) and (c) are the single-shot images from the red and blue fluorescence cameras captured simultaneously with (a), (d) is the intensity ratio image, (e) is the temperature image

was found to vary by less than 5%, no correction for laser power was applied. Fluorescent images were processed using in-house Matlab scripts. First, the images were corrected for background noise by subtracting mean images taken under experimental conditions without toluene or particles in the flow. They were then corrected for individual pixel collection efficiency using images of a diffuse UV lamp and spatially aligned by matching corresponding points on the red, blue and interference images. The images were then thresholded to remove areas of low signal, before the ratio of the recorded intensity in the red image to the blue image was found for corresponding pixels in each image. Each pixel of the intensity ratio image was converted to temperature with a calibration curve.

Results

The relationship between intensity ratio and temperature was determined by calibration, because this relationship is unique for each system and dependent on each camera, the optical filters used in the red and blue channels and the laser. The calibration was performed in the same wind tunnel in a flow without particles. The flow in the central pipe was heated with the electrical tape heater at a constant voltage while running a toluene-seeded nitrogen flow until the temperature reached a steady state. The voltage was varied to set the pipe temperature in the range of 15-215°C. Two thermocouples were used to monitor the temperatures of the pipe wall and the gas within the pipe, just upstream from the exit. When the thermocouple readings of the gas flow and pipe reached steady state, 250 fluorescence images of the flow were taken. From the images, the mean intensity ratio value in a region within the potential core

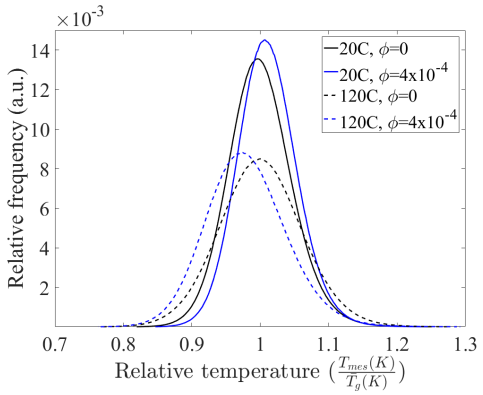

Figure 5: Histogram of temperature measurements of pixels binned 9×9 for all images

of 140×45 pixels (4.6×1.5 mm) was averaged over all images to find the relationship between intensity ratio and temperature. The intensity ratio was measured in a region where there was no interference from the thermocouple probe on the image. The standard deviation of individual pixels in the mean image was ± 6°C at room temperature and ± 15°C at 215°C.

Figure 3 presents the dependence of I_{Red}/I_{Blue} on the gas temperature as measured with the thermocouple. The results show that the intensity ratio increases with temperature, with a near linear relationship. This is consistent with the data presented by [11] in this temperature range for a different filter combination. The results also show that the fluorescence emission at both wavelengths decrease with temperature. This is due to the decrease in fluorescence quantum yield of toluene with temperature [6]. The average signal to noise ratio (SNR), defined as the ratio of total signal with toluene to the signal in the background images, was measured to be 14.2 at room temperature for the red camera, decreasing to 4.8 at 215°C. The blue camera had a SNR of 25.1 at room temperature and 5.0 at 215°C. A quadratic relationship was chosen as it gave the best fit to the data from the calibration. The intensity of the fluorescent emission does not follow a smooth curve in the calibration data as experimental conditions such as toluene concentration and laser power were not constant throughout the calibration. However, these variations did not affect the intensity ratio measurement, which confirms that a ratio method is suitable for experiments under these conditions. The calibration curve used to convert from intensity ratio (IR) to temperature was $T = 94.58IR^2 + 338.6IR - 198.3$, with T here the temperature in Celsius.

Examples of single-shot images recorded simultaneously are presented in figure 4, showing the red (b) and blue (c) fluorescence images, together with the particle image (a) providing a measure of both particle number density and interference. The structure of the turbulent jet can be seen in the fluorescence images, with the fluorescent signal intensity being strongest on the jet centreline and near the jet exit plane, as expected. The signal decreases downstream and away from the centreline due to mixing of the central jet with the annular nitrogen flow. The blue and red images were matched pixel by pixel to obtain the intensity ratio image (d). The ratio image was then converted to temperature (e) using the calculated calibration curve. The images shown in figure 4 were taken with particles at an instantaneous loading $\phi_v \approx 4\text{x}10^{-4}$. Importantly the particles that are clearly evident from the interference image have no visible impact on the fluorescence images.

Figure 5 presents histograms of temperature measurement binned in 9×9 pixel regions of single-shot images of the flow

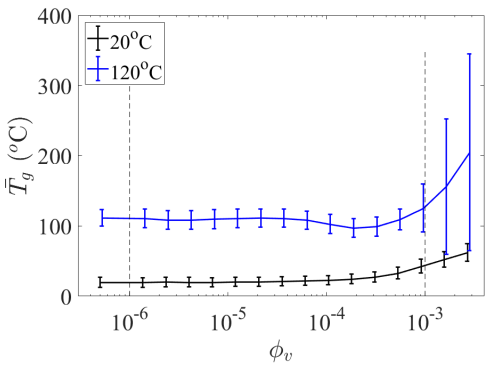

Figure 6: Effect of particle loading on mean temperature calculation. Error bars show one standard deviation either side of the mean value. The dashed vertical lines indicate the boundaries of the two-way coupling regime

without particles and with an instantaneous particle loading between $2\times10^{-4} < \phi_v < 8\times10^{-4}$, at pipe temperatures ($T_p$) of 20°C and 120°C. At $T_p = 20$°C in the flow without particles the mean gas temperature ($\bar{T}_g$) recorded was 19.9°C, with a standard deviation of 14°C. In the flow with particles, $\bar{T}_g$ increases to 23.1°C, however the standard deviation is similar, at 13°C. At $T_p = 120$°C, $\bar{T}_g$ in the flow without particles was 107.4°C, with a standard deviation of 23.7°C. $\bar{T}_g$ is not equal to T_p due to the gas not reaching an equilibrium state in the heating section, and the standard deviation is greater as the fluorescent signal strength is lower at high temperatures. At 120°C with particles, $\bar{T}_g$ decreases to 99.6°C, with a standard deviation of 23.5°C. This shift in mean temperature could be due to the combination of a lower temperature of the flow and interference of particles on the measurement.

Figure 6 presents the measured temperature as a function of ϕ_v for the two gas temperatures of 20°C and 120°C. The temperature and particle loading were measured from 9×9 bins of locations of strong signal in the jet, with the width of the total measurement region based on the pipe diameter at the jet exit and the length being from the jet exit to near the downstream edge of the image. It can be seen that $\bar{T}_g$ is independent from ϕ_v for $\phi_v < 5\text{x}10^{-4}$ at 20°C and for $\phi_v < 2\text{x}10^{-4}$ at 120°C. Possible causes for the interference that occurs for $\phi_v > 5\text{x}10^{-4}$ are (i) that the optical filters do not completely remove the high intensity elastically scattered laser light from particles, (ii) secondary excitation of toluene that is not in the measurement region by laser light scattered from the particles, (iii) fluorescence of the particles, or (iv) the actual temperature of the flow not reaching equilibrium the pipe at high particle loadings. Further work to identify these causes may allow the measurement to be extended to even higher volumetric loadings.

Conclusions

The effect of adding 40 μm PMMA particles on the PLIF thermometry method with toluene as the tracer was investigated. The method was found to measure gas temperatures to within 10°C for mean particle volume loadings of $\phi_v < 5\times10^{-4}$ at 20°C and $\phi_v < 2\times10^{-4}$ at temperatures of 120°C for the conditions investigated here. These loadings are in the two-way coupling regime, which is of interest in some industrial systems. Interference from the particles was found to be significant for particle volume loadings of $\phi_v > 10^-3$, which indicates that more work is required to extend the method for use in the 4-way coupling regime.

Acknowledgements

The authors would like to acknowledge the financial contributions of the Australian government through the Australian Research Council (Discovery grant 150102230 and Linkage Grant LE130100127)

References

[1] Antonia, R. and Mi, J., Temperature dissipation in a turbulent round jet, *J. Fluid Mech*, **250**, 1993, 531–551.

[2] Elghobashi, S., An Updated Classification Map of Particle-Laden Turbulent Flows, *IUTAM Symp. on Comp. Mult. Flow*, editors S. Balachandar and A. Prosperetti, 2006

[3] Faust, S., Goschütz, M., Kaiser, S., Dreier, T. and Schulz, C., A comparison of selected organic tracers for quantitative scalar imaging in the gas phase via laser-induced fluorescence, *App. Phys. B*, **117**, 2014, 183–194.

[4] Ho, C. and Iverson, B., Review of high-temperature central receiver designs for concentrating solar power. *Renew. and Sustain. Energy Rev.*, **29**, 2014, 835–846.

[5] Incorpera, F., *Fundamentals of heat and mass transfer*, Wiley, 2007

[6] Koban, W., Koch, J., Hanson, R. and Schulz, C., Absorption and fluorescence of toluene vapor at elevated temperatures, *Phys. Chem. Chem. Phys.*, **6**, 2004, 2940–2945.

[7] Koban, W., Koch, J., Hanson, R. and Schulz, C., Oxygen quenching of toluene fluorescence at elevated temperatures, *Appl. Phys. B*, **80**, 2005, 777–784.

[8] Kristensson, E., Ehn, A., Bood, J. and Aldén, M., Advancements in Rayleigh scattering thermometry by means of structured illumination, *Proc. Combust. Inst.*, **35**, 2015, 3689–3696.

[9] Lau, T. and Nathan, G., Influence of Stokes number on the velocity and concentration distributions in particle-laden jets, *J. Fluid Mech*, **757**, 2014, 432–457.

[10] Lau, T. and Nathan, G., The effect of Stokes number on particle velocity and concentration distributions in a well-characterised, turbulent, co-flowing two-phase jet, *J. Fluid Mech*, **809** 2016, 72–110.

[11] Luong, M., Koban, W. and Schulz, C., Novel strategies for imaging temperature distribution using Toluene LIF, *J. Phys.: Conference Series*, **45**, 2006 133–139.

[12] Miller, F. and Koenigsdorff, R., Theoretical analysis of a high-temperature small-particle solar receiver, *Solar Energy Materials*, **24**, 1991, 210–221.

[13] Miller, J., Slipchenko, M., Mance, J., Roy, S. and Jord, J., 1-kHz two-dimensional coherent anti-Stokes Raman scattering (2D-CARS) for gas-phase thermometry, *Optics Express*, **24**, 2016 24971–24979.

[14] Schulz, C. and Sick, V., Tracer-LIF diagnostics: quantitative measurement of fuel concentration, temperature and fuel/air ratio in practical combustion systems, *Prog. Energy Combust. Sci.*, **31**, 2005, 75–121.

[15] Williams, A., Pourkashanian and Jones, J.M., Combustion of pulverised coal and biomass, *Prog. Energy Combust. Sci.*, **27**, 2001, 587–610.